International Journal of Pharmaceutics 494 (2015) 152–166

Contents lists available at ScienceDirect

International Journal of Pharmaceutics

journal homepage: www.elsevier.com/locate/ijpharm

The parameters influencing the morphology of poly(ε-caprolactone) microspheres and the resulting release of encapsulated drugs

Jessica Bile[a], Marie-Alexandrine Bolzinger[a], Charlène Vigne[a], Olivier Boyron[b], Jean-Pierre Valour[a], Hatem Fessi[a], Yves Chevalier[a,*]

[a] Université Claude Bernard Lyon 1, Laboratoire d'Automatique et de Génie des Procédés (LAGEP), CNRS UMR 5007, 43 bd du 11 Novembre, 69622 Villeurbanne, France
[b] Université Claude Bernard Lyon 1, Laboratoire de Chimie et Procédés de Polymérisation (C2P2), CNRS UMR 5265, CPE, 43 bd du 11 Novembre, 69622 Villeurbanne, France

ARTICLE INFO

Article history:
Received 4 May 2015
Received in revised form 24 July 2015
Accepted 26 July 2015
Available online 30 July 2015

Keywords:
Microencapsulation
Morphology
Drug release
poly(ε-Caprolactone)
Cholecalciferol
In situ video probe

ABSTRACT

Polymer microparticles used for drug encapsulation and delivery have various surface morphologies depending on the type of formulation ingredients and parameters of the manufacture process. This works aims at investigating the critical parameters governing the morphology of microparticles and to underline the influence of their surface state on the drug release. The classical fabrication process by the "emulsion–solvent evaporation" is addressed using poly(ε-caprolactone) as the polymer and methylene chloride as the volatile organic solvent. The typical surfactants poly(vinyl alcohol) and polysorbate 80 have been considered. Scanning electron microscopy observations showed the various surface morphologies mainly depending on the stirring rate, the viscosity of the oil phase and by the presence of inappropriate surfactants. Because of arrested coalescence during solvent evaporation, the evaporation of the organic solvent causing particles hardening is the most important parameter that controls the morphology. Indeed, slow evaporation allows partial coalescence of the soft particles swollen by the organic solvent, whereas the particles morphology is frozen rapidly upon fast evaporation, thus preventing damaged surface states. Moreover, an effective stabilizing system for the primary emulsion is also a determining factor to control the final morphology. The morphology of the particles has a definite influence on the drug delivery of cholecalciferol. The surface morphology should be taken into consideration in the design of polymer microparticles because it allows a control over the drug release kinetics.

1. Introduction

Microencapsulation has been used for a long time in the pharmaceutical field because of its obvious advantages, such as the drug protection and controlled delivery. The resulting targeting and prolonged treatment reduces the systemic concentration of drugs and allows decreasing the administration frequency, leading to decreased side effects and improved patient convenience (Dhanarajua et al., 2010). To reach such achievements, microencapsulation using the oil/water (o/w) emulsion/solvent evaporation technique is common owing to its easy implementation (Kim et al., 2005). It has enabled the encapsulation of numerous lipophilic active agents such as nifedipine or progesterone (Sansdrap and Moës, 1993; Benoit et al., 1986). Encapsulation has improved the activity of vitamin D_3 (cholecalciferol) that is very sensitive to degradation and needs a protection against the environment (Petritz et al., 2006; Gonnet et al., 2010; Almouazen et al., 2013). The polymer materials used for pharmaceutical applications are most often aliphatic polyesters, such as the poly(lactic acid) (PLA), poly(lactic-*co*-glycolic acid) (PLGA) and poly(ε-caprolactone) (PCL) because of their biocompatibility and biodegradability (Wiscke and Schwendeman, 2008).

Typical formulation and processing parameters of the conventional microencapsulation process by o/w emulsion/solvent evaporation are the polymer molar mass and concentration, the drug/polymer ratio, the surfactant type, and the speed and shear rate of the agitation system (Li et al., 2008; Benoit et al., 1999; Zhu et al., 2005; Sansdrap and Moës, 1993; Jeyanthi et al., 1997). The impact of these factors on microspheres size, drug loading and drug release is well-documented (O'Donnell and McGinity, 1997). Nevertheless, researches concerning the microparticles surface state are scarce and the influence of each parameter is not well understood. It has been reported that deteriorated morphologies were obtained in case of evaporation under reduced pressure due to the

* Corresponding author. Tel.: +33 472431877.
E-mail address: chevalier@lagep.univ-lyon1.fr (Y. Chevalier).

http://dx.doi.org/10.1016/j.ijpharm.2015.07.068
0378-5173/

amorphous state of the polymer matrix (Izumikawa et al., 1991; Chung et al., 2001). Dubernet et al. (1987) also noticed that the surface state was related to the microspheres size.

Among the aliphatic polyesters available, the polycaprolactone has been under most of the investigations because its degradation is slow and does not generate an acidic environment (Dash and Konkimalla, 2012; Woodruff and Hutmacher, 2010). Slow degradation enables long term sustained drug release (Sinha et al., 2004). However, PCL microspheres resulting from the o/w emulsion/solvent evaporation process exhibited some rough (Suave et al., 2010), or pitted morphologies (Dordunoo et al., 1995), with surfaces containing big holes (Zhu et al., 2005) and deep cracks (Dubernet et al., 1987). Deteriorated morphologies have just been noticed in most instances and, to the best of our knowledge, their formation has rarely been investigated in details. Indeed, most publications focused on drug release better than morphology. Nevertheless, the drug release is strongly correlated to the surface state. Indeed, damaged morphologies showing pores and craters were correlated with faster drug release (Le Ray et al., 2003; Kishida et al., 1990; Freiberg and Zhu, 2004; Yang et al., 2001). As a consequence, even if the morphological behavior of PCL microparticles is poorly addressed in the literature, it has been found to be an important parameter.

To design biodegradable polymeric microspheres with the desired drug release profile it seems worth identifying the factors that impact the morphology for the commonly used poly(ε-caprolactone) microparticles prepared by the emulsion/solvent evaporation technique. The present contribution purposes to discuss the causes of morphological damages with respect to the formulation and process parameters, such as the dispersed phase viscosity, the agitation system, and the type of surfactants in the emulsification process. Typical surfactants like poly(vinyl alcohol) (PVA) and polysorbate 80 and the most commonly used solvent dichloromethane (DCM) were used in order to match to the general framework of most previous studies (Kim et al., 2005; Li et al., 2008). Blank microparticles were studied in a first step in order to understand the morphological phenomenon without active agent. Then, loaded microparticles with cholecalciferol were formulated without modification of the expected surface state in order to study the relationships between the surface state and the drug release. Cholecalciferol has an antitumoral activity in supraphysiological conditions (Gross et al., 1998) and its targeted sustained delivery enables the administration of effective serum concentration without risk of hypercalcemia. Cholecalciferol has been selected in the present study because there are obvious advantages of its encapsulation in a sustained drug delivery system. Encapsulation is an interesting solution for administration of cholecalciferol and several studies have previously been reported on this subject proving that encapsulation enhances the drug activity (Almouazen et al., 2013; Gonnet et al., 2010; Petritz et al., 2006). It is also an appropriate candidate for further studies of the effect on the skin for the *keratinocyte differentiation*.

2. Materials and methods

2.1. Materials

The two poly(ε-caprolactone) (PCL) polymers of number-average molar masses M_n 45,000 and 80,000 Da were denoted as PCL_{45000} and PCL_{80000} in the following. PCL_{45000}, PCL_{80000}, poly(vinyl alcohol) (PVA) of hydrolysis rate 86.7–88.7% and weight-average molar mass M_w 31,000 Da, and dichloromethane (DCM) of reagent grade were purchased from Sigma-Aldrich. Polysorbate 80 was from Fisher Scientific. Cholecalciferol (vitamin D3) of 99% purity was from Alfa Aesar. All other reagents were reagent grade and used as supplied.

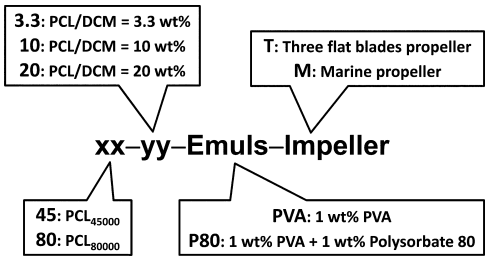

Fig. 1. Abbreviation codes for the batch names.

2.2. Preparation of microspheres

In a first step, an o/w emulsion was prepared with a mass ratio between the organic and aqueous phases of 1/10. The aqueous phase (300 g) contained 1 wt% of PVA as stabilizer (and 1 wt% of polysorbate 80 in some experiments). For blank microparticles, the organic phase was a solution of either PCL_{80000} or PCL_{45000} dissolved in 30 g of DCM at various polymer/solvent mass ratios: 3.3, 10 and 20 wt%. For loaded microparticles, cholecalciferol was added in the organic phase in order to obtain a loading capacity DL = 2 wt%. The drug loading capacity and encapsulation efficiency of cholecalciferol were calculated as follows (Gupta and Kumar, 2001; Huang et al., 2010):

$$\text{drug loading capacity : DL} = \frac{\text{mass of cholecalciferol in the PCL particles}}{\text{mass of PCL}} \quad (1)$$

$$\text{encapsulation efficicency : EE} = \frac{\text{mass of cholecalciferol in the PCL particles}}{\text{total mass of added cholecalciferol}} \quad (2)$$

The emulsion was prepared by pouring the organic phase in the aqueous phase under stirring. Different stirrers were used: a three flat blades propeller of 40 mm diameter at the rotation rate of 860 rpm or a marine propeller of 38 mm diameter at the rotation rate of 500 rpm. The emulsions were left 4 h under the same stirring conditions at room temperature and atmospheric pressure to allow for the DCM evaporation. The resulting solid microspheres were filtered and air-dried overnight at room temperature. The abbreviations of the batches are given in Fig. 1.

2.3. Particle size analysis

The size distributions of emulsion droplets and microspheres were characterized by laser light scattering (Mastersizer 2000, Malvern, UK). For the size measurement of the emulsion droplets, the dilution medium was composed of a surfactant solution (PVA 1 wt% or PVA 1 wt% + polysorbate 80 1 wt% depending on the experiment) in water saturated with DCM. For the size measurements of the microspheres, the dilution medium was pure water. The particle size distribution was calculated from the scattered intensity using the Fraunhofer theory which is valid for the large particle size of the present study. The average of triplicate measurements for each batch was made. Particle sizes were expressed as the average diameter (Sauter diameter, $d_{3,2}$).

2.4. In situ monitoring the emulsions with the video probe

In situ monitoring of the microencapsulation process according to the formulations described in Table 1 was performed using the video probe EZ PROBE D25 L12001 designed in our laboratory. Such

Table 1
Effect of the PCL concentration and molar mass on the mean diameters of the emulsion droplets and dry microparticles.

Sample	Emulsion droplet mean diameter (μm)	Mean diameter of dry microparticles (μm)	
		Calc. from Eq. (2)	Measured
Three flat blades propeller			
45-3.3-PVA-T	22	7	20
45-10-PVA-T	39	18	41
80-3.3-PVA-T	50	16	45
80-10-PVA-T	416	193	350
Marine propeller			
45-3.3-PVA-M	61	20	56
45-10-PVA-M	80	37	105
80-3.3-PVA-M	92	30	132
80-10-PVA-M	580	270	530

video probe records pictures of emulsion droplets, polymer particles, crystalline particles inside the stirred vessel (Gagnière et al., 2009; Khalil et al., 2010, 2012; Ach et al., 2015). Such instrument allows imaging the particles *in situ* during the course of the process. As an obvious benefit, it allows observations of unstable particles inside the stirred vessel, without having to stop the agitation or to sample out an aliquot. The probe was immersed in the vessel and enabled the recording of real time 2D images of the dispersion at the rate of 50 frames per second. It was equipped with back-lighting making the droplets black on a white background.

2.5. Scanning electron microscopy

The shape and surface state of microparticles as well as the internal morphology were studied using scanning electron microscopy (SEM) (Neoscope, JCM-5000, JEOL, Japan). 10 mg of dried microparticles were suspended in 5 mL of ultra-pure water. A drop of this suspension was deposited on a double-sided adhesive carbon paste tape stuck onto an aluminum stub. After drying, it was vacuum coated with a 20 nm thickness platinum film under an argon atmosphere. Samples were directly observed with SEM in high vacuum mode using an acceleration voltage of 10 kV. The internal morphology of microparticles was observed after freeze-fracture with a microtome either in liquid nitrogen, or at −80 °C, or at −40 °C.

2.6. Evaporation rate of dichloromethane

The evaporation rate of DCM was measured by weighing the microparticle suspensions under stirring every 3 min. The mass loss was determined by comparing the mass measured at a given time to the initial mass. The same experiment using only aqueous phase with the same agitation system was used as control. It has been proved that the solvent evaporation profile was linear at short durations, so that the evaporation rate was constant and could be described by the following equation based on Fick's law (Eq. (1); Li et al., 2008)

$$\frac{dM}{dt} = -AKC_s \tag{3}$$

where M is the solvent total mass in the reactor (kg), t the time (s), A the surface area (m^2) of the air–water interface, K is the evaporation rate constant ($m\,s^{-1}$), and C_s is the solvent concentration in the continuous phase ($kg\,m^{-3}$). The evaporation rate has been determined from the slope of the mass loss with respect to time during the first 15 min of the evaporation process.

2.7. Viscosity measurements of the oil phase

The viscosity of the different organic phases was determined without cholecalciferol using a rotational rheometer (Modular Compact Rheometer 302 Anton Paar, Austria). Steady-shear viscosity measurements were performed at 20 °C with a cone-and-plate geometry (0.997°, diameter 50 mm). Shear stress measurements were carried out in experiments where the shear rate ($\dot{\gamma}$) was increased stepwise from 0.1 to 300 s^{-1} in 60 s.

2.8. Measurement of interfacial tension by the pendant drop method

The interfacial tension between the aqueous and organic phases of the emulsion was measured by the pendant drop method (Drop Shape Analysis DSA10M122, Krüss, Germany) at ambient temperature. Pendant drops were suspended at the tip of a 0.5 cm diameter stainless steel needle in a glass cell filled with 5 mL of pure water or water containing various surfactants. The interfacial tension was determined from the drop profile using the Laplace equation (Girault et al., 1984). The aqueous phase contained the surfactant and the organic phase was a 3.3 wt% solution of PCL_{80000} in DCM.

2.9. Surfactant partition coefficient

The partition coefficient of the surfactant between the aqueous and oil phases was measured in triplicate by introducing 1 wt% of polysorbate 80 or PVA in 6 mL of water and 6 mL of DCM previously saturated with each other. The mixture was stirred magnetically for 5 h at ambient temperature and the phases were separated by centrifugation (Centrifuge 5430, Eppendorf, Germany) for 20 min at 7000 rpm which corresponded to relative centrifugal force of 5752 × g in order to break the emulsion. Each phase was collected and analyzed for the surfactant concentration by thermogravimetry.

2.10. Determination of drug loading

100 mg of microparticles were introduced in 10 mL acetonitrile. The mixture was left for 3 h under stirring and then filtered through a 0.45 μm syringe filter. The samples were analyzed for cholecalciferol content using high-pressure liquid chromatography with a reverse phase column. The HPLC set up from Agilent (France) was composed of a Agilent 717 injector, an Agilent pump, a reverse phase column X-Terra MS C18 column (5 μm, 4.6 × 250 mm) and a photodiode array UV detector working at 265 nm wavelength. The elution with methanol/acetonitrile/acetic acid 0.5% (85:10:5) solvent at 1.3 mL min^{-1} flow rate and 30 °C gave a retention time of 5.12 min for cholecalciferol. The calibration curve for quantitative analysis was linear up from 0.1 to 5 μg mL^{-1} (r^2 = 0.999) (Almouazen et al., 2013). The drug loading was defined as the ratio of the drug mass to the mass of dry microparticles.

2.11. Drug release experiments

In vitro release of cholecalciferol was measured by introducing 50 mg of drug loaded microparticles in 50 mL phosphate buffered saline (PBS 0.01 M, pH 7.4) containing 0.1 wt% sodium dodecyl sulfate (SDS) to increase the cholecalciferol solubility and ensure sink conditions (the maximum final concentration of drug was 20 $\mu g\,mL^{-1}$). The medium was stirred at a moderate rate of 150 rpm at 37 °C for 10 days. For everyday analysis of release of cholecalciferol, agitation was stopped and the sedimentation of microparticles was performed by centrifugation (2000 × *g*, 10 min). 4 mL of supernatant was collected, filtered through a 0.45 μm membrane filter and analyzed by RP-HPLC using the previously mentioned HPLC method. The volume removed was replaced by fresh phosphate buffer for resuming the release experiment (Almouazen et al., 2013).

3. Results

Morphologies of blank PCL microparticles obtained from o/w microencapsulation by solvent evaporation were observed by SEM and sorted in different classes. The aim was to determine the parameters of relevance to the control of the various surface morphologies. For this purpose, the mechanism of formation of the various surface morphologies was investigated and the influence of the several parameters of relevance such as the speed and shear rate of the agitation system, the polymer molar mass, the polymer concentration in the organic phase, and the use of surfactants were investigated. All of them influenced the solvent evaporation rate that enabled the liquid emulsion droplets to convert into solid microspheres. After studying the influence of each parameter on the morphology, the release of the cholecalciferol was studied for microparticles having different morphologies in order to estimate the impact of the surface state on drug release.

3.1. Microsphere morphologies

Five different morphologies (Fig. 2) that have already been observed in previous works were observed: smooth surface, dumbbells, scars and defects (Jeong et al., 2003; Dubernet et al., 1987), roughness (Suave et al., 2010), and surface states with holes (Dordunoo et al., 1995; Perez et al., 2000; Dubernet et al., 1987; Zhu et al., 2005).

The surface morphologies have been sorted into five different classes as smooth, rough, scarred, dumbbell-shaped, and holy. This is descriptive only. Since it was aimed to sort them according to their formation process and to discuss the influences of the formulation and process parameters, the different morphologies have been associated to a hypothetic formation mechanism. Various formation mechanisms have been postulated for each type of morphology, and complementary experiments have been performed as a validation of the hypotheses. The presumed scenarii are the following:The smooth surface is the most often expected morphology since it corresponds to the idealistic idea of the mechanism taking place by emulsification into spherical droplets containing the solution of PCL in DCM, followed by an isotropic exit of DCM causing an isotropic shrinkage of the droplets during the solvent evaporation stage. However coalescence of liquid droplets retains the smooth spherical shape and may result in the same smooth final morphology.The formation of dumbbells obviously came from the merging of two droplets that has been arrested before the spherical shape could be recovered because of fast particle hardening. The origin of dumbbell formation was therefore coagulation of emulsion droplets followed by partial coalescence. Coalescence has been stopped because DCM evaporation was faster that coalescence.The morphology of scarred particles is close to that of dumbbells. Coalescence just went further but it did not reach completion. More than two droplets have possibly stuck together. Complete coalescence would give rise to the smooth morphology.The rough morphology corresponded to the attachment of many small droplets to a larger one followed by their arrested coalescence. This again requires that coagulation (flocculation) occurred and coalescence have been stopped by fast hardening due to fast DCM evaporation.The holy morphology was clearly different. Pinholes and large cracks were observed. It was thought that a rigid crust of PCL formed at the surface of the droplets. DCM remaining in the core of the droplets caused the crust to rupture for further removal of DCM as the evaporation proceeded.

As a whole, there were only two postulated mechanisms of formation of defects at the surface of microparticles: (i) coagulation and arrested coalescence that caused dumbbells, scars and surface roughness; (ii) fast drying of the surface of the droplets causing the formation of a PCL crust encapsulating residual DCM and subsequent rupture of this impermeable PCL film. According to the later mechanism of holes formation, the dry microparticles should have a large cavity in their center behind the hole by which the encapsulated DCM could leak. This was indeed the case since observations of the internal structure of holy microparticles by SEM of either microtome-cut or freeze-fractured microparticles revealed the presence of voids inside the microparticles (Fig. 3). Microparticles 45-10-PVA-T which had scars and showed very few pinholes at their surface had small voids in their center. Some such voids were adjoining the surface holes and others formed a closed porosity. The observed closed pores indicated that the cracks by which DCM could leak off the droplets have healed before completion of the microparticles hardening. Microparticles 45-20-PVA-T having a large density of holes at their surface were highly porous; large voids were indeed observed by SEM after freeze-fracture.

3.2. Assessment of the main mechanisms causing non-spherical particle shapes

The emulsion/solvent evaporation process consists in two stages: emulsification followed by solvent evaporation. Once the emulsion has been prepared, solvent evaporation of the DCM content of each droplet should cause shrinkage of each droplet such that its volume (and diameter) was reduced according to the PCL/DCM ratio. In the “ideal case” where each emulsion droplet shrunk independently so as to yield a dry polymer microparticle at the end of the solvent evaporation stage, the microparticle sizes d_{part} could be calculated from the emulsion droplet size d_{32} and polymer concentration in the oil phase from simple geometrical considerations as

$$d_{part} = d_{32}(\phi_{PCL})^{1/3} \quad (4)$$

where ϕ_{PCL} is the volume fraction of PCL in the oil phase. The experimental data reported in Table 1 did not follow such an ideal behavior. The experimental diameters of dry microparticles were much larger than those predicted from the emulsion droplet size and Eq. (4) (Table 1). Obviously, coalescence took place during the solvent evaporation stage. Droplets coalescence during solvent evaporation has been inferred from the observations of scarred and rough surface morphologies of the microparticles. It was confirmed from the comparison of the droplet and microparticles sizes. Even microparticles having a smooth spherical surface had a size larger than predicted assuming individual drying of oil droplets, showing that coalescence did occur in every instance.

The arrested coalescence phenomenon could be observed in the stirred tank during the solvent evaporation stage by using the *in situ* video probe. Thus, Fig. 4 shows instances of such oil

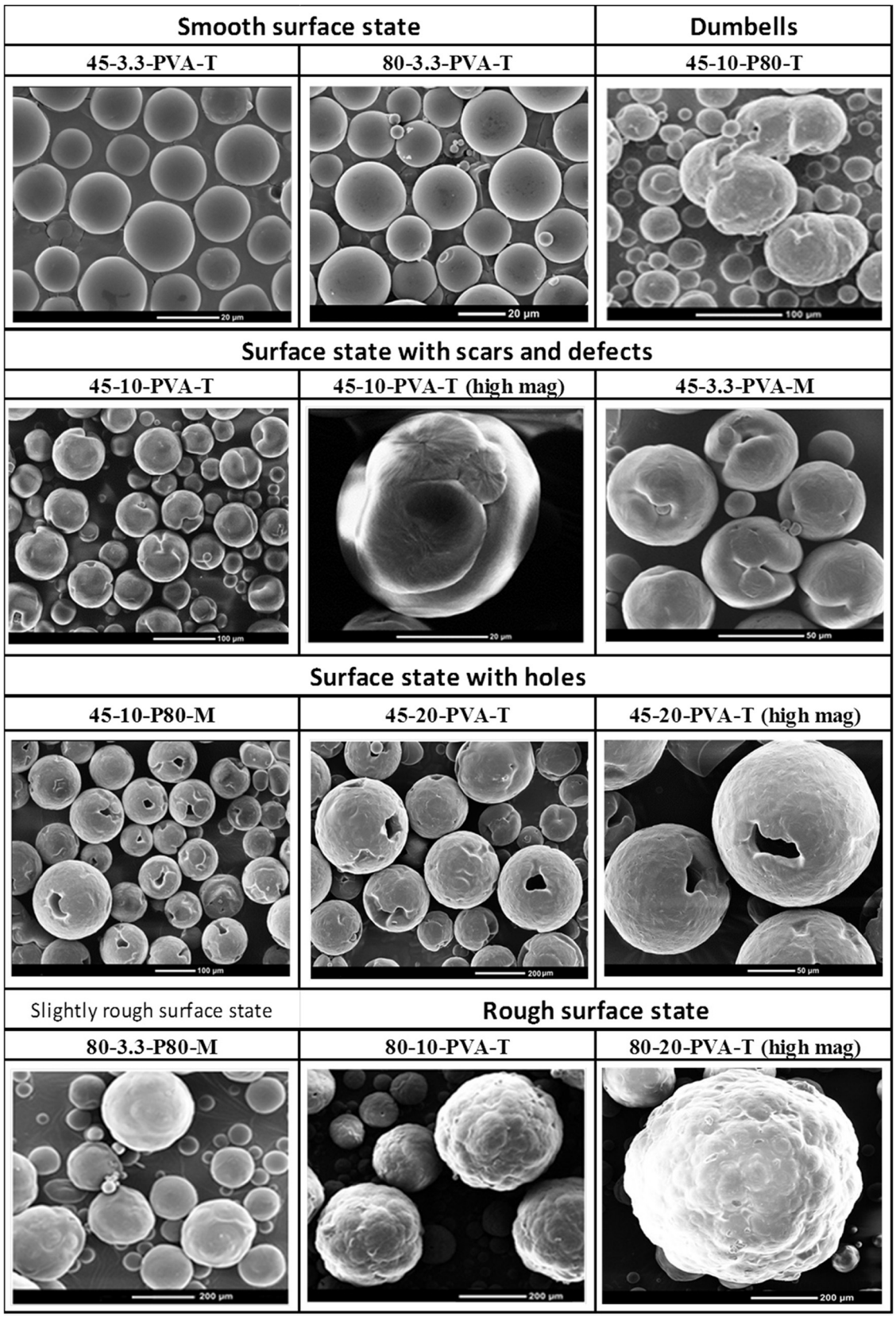

Fig. 2. SEM pictures of PCL microparticles illustrating the different morphologies obtained in various experiments.

droplets undergoing coalescence in the stirred tank, leading to non-spherical final morphologies of the microparticles, dumbbell, scars or rough surfaces. It has been inferred in several previous reports that non-spherical morphologies of the microparticles came from oil droplets or microparticles sticking together because of the tackiness of their surface (Jalil and Nixon, 1990). The direct observations by the video probe and the final morphologies did not match to this idea. There was clear evidence of a coalescence of the oil

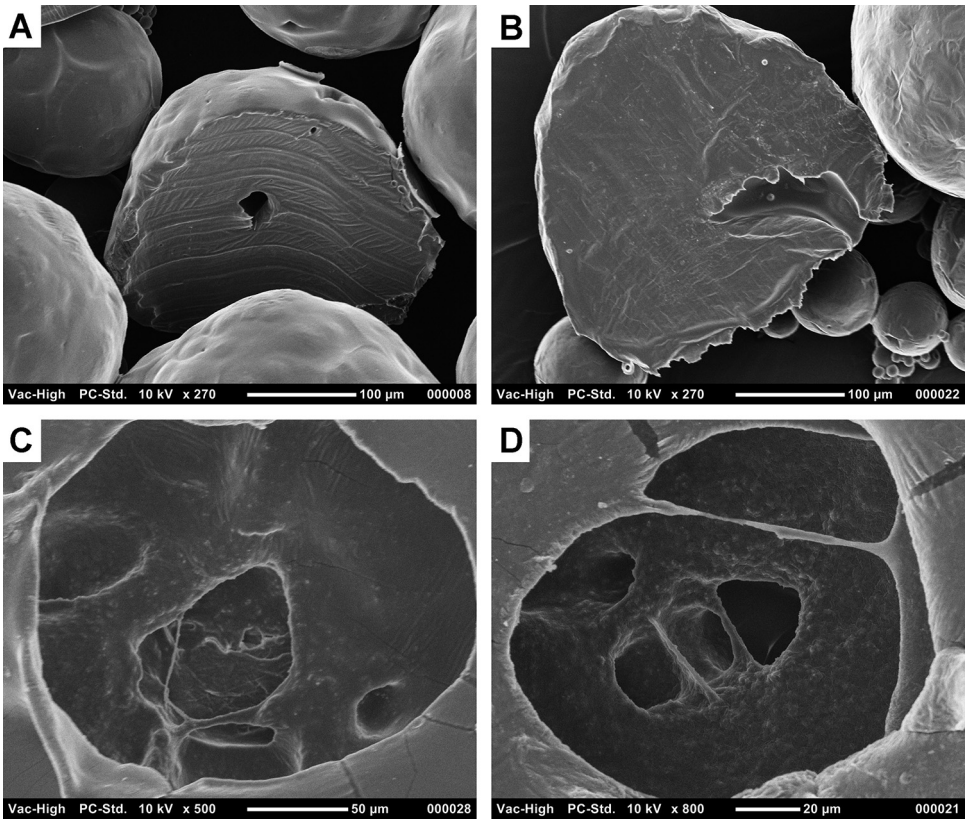

Fig. 3. SEM pictures of the internal structure of fractured holy PCL microparticles showing the presence of large cavities behind the surface holes. (A and B) Microparticles of 45-10-PVA-T cut with a microtome at −45 °C showing the presence of voids in the center of the particles; picture B shows a void adjoining a hole at the surface of the microparticles. (C and D) Freeze-fractured microparticles of 45-20-PVA-T showing the large voids in case of extensive formation of holes and cracks at the surface of microparticles.

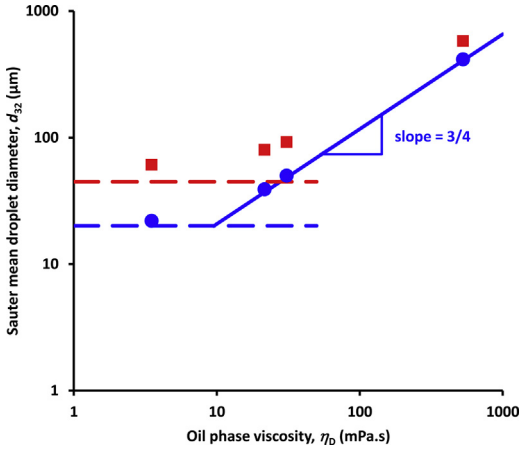

Fig. 4. Pictures of coalescence phenomena observed *in situ* with the video probe. The arrows show the droplets under coalescence events (For interpretation of the color information in this figure legend, the reader is referred to the web version of the article.).

droplets during the drying stage. The difference between "coagulation", "sticking", and "coalescence" is not only a semantic matter. "Coagulation" or "flocculation" is a phenomenon where oil droplets coming into contact each other because of attractive forces operating between oil droplets. As a result of coagulation, oil droplets are aggregated but they are still intact since there is still the surfactant stabilizing layer remaining at the surface of each droplet, even in the between the surface of contact between droplets. Coagulation can be reversible in case where stirring causes shear forces stronger than the attractive force between droplets. "Sticking" involves a direct contact between the tacky materials of each particle, so that the surfactant layer that remained after the coagulation should have been shifted off. "Coalescence" is a mixing process of the oil contents of contacting droplets. Two spherical liquid droplets merge into a single spherical droplet when coalescence goes to completion. In case where the oil phase is highly viscous, coalescence can be stopped before single droplets could reach the final spherical shape. This process called "arrested coalescence" causes the formation of the present non-spherical particle shapes. Oil droplets mix during coalescence because oil is liquid. Sticking does not involve mixing of the droplets; the materials at the particles surfaces just mix on a molecular scale.

So as to investigate the influence of the process parameters, the following physicochemical experiments were carried out. Since the competition between coalescence and solvent evaporation during the solvent evaporation stage controlled the morphology of the arrested coalescence states, the DCM evaporation rate was first measured. The rate at which solid polymer microparticles formed from emulsion droplets depended on the DCM evaporation rate and the rate at which DCM diffused out of emulsion droplets. The later process depended on the droplet size controlled by the stirring process and the viscosity of the oil phase. The emulsion prepared in the first stage of the emulsion/solvent evaporation process was characterized for the droplet size, the parameters that control such size (the stirring process and the viscosity of the oil phase), and the stability of the emulsion with regards to coagulation and coalescence. The parameters that controlled the morphology of the microparticles were several and contributed in several ways. In particular, the viscosity of the oil phase set by the molar mass of PCL and the concentration in DCM influenced the droplets size during the emulsification stage and the diffusion of DCM out of

Table 2
Influence of the experiment formulation and processing parameters on the solvent evaporation rate.

Experiment	DCM evaporation rate (g min^{-1})
45-3.3-PVA-T	0.91
45-3.3-PVA-M	0.27
45-3.3-P80-M	0.43
45-10-PVA-T	0.71
80-3.3-PVA-T	0.80
80-3.3-PVA-M	0.20
80-3.3-P80-M	0.35
80-10-PVA-T	0.41

the droplets during the evaporation stage. The final size of the dry microparticles depended on both the droplet size of the emulsion and the PCL concentration in the oil phase, so that the contributions of the parameters were quite intricate. Finally, the influence of type of emulsifier was addressed because unexpected results were observed in the presence of polysorbate 80.

3.3. Study of the evaporation rate of DCM

DCM evaporation occurs in four successive steps including two transfers through an interface: the oil–water and the water–gas interfaces. The two interfacial transfer rates depend on the stirring conditions. Indeed stirring leaves a stagnant layer close to the surface at which DCM transfer takes place. The transfer of DCM from the emulsion droplets to the aqueous phase and from the aqueous phase to the gas phase takes place through the stagnant layer by passive diffusion driven by the gradient of chemical potential between the two phases. The transfer rate depends on the thickness of the stagnant layer that is controlled by the stirring efficiency. First, DCM diffuses from the core of the droplets to their surface; such a passive diffusion step does not depend on the agitation. Diffusion of DCM inside the droplets depends on their size and the viscosity of the oil phase. Next, DCM is transferred from the emulsion droplets surface into the aqueous phase by diffusion through the stagnant layer. Thirdly DCM present in the bulk of the aqueous phase should reach its top surface where evaporation takes place. Such a transport of DCM in the aqueous phase is ensured by stirring. Finally, DCM crosses through the stagnant layer at the top surface of the emulsion for evaporation can take place. Such fourth step is again controlled by the stirring conditions that set the thickness of the stagnant layer. The overall rate of DCM evaporation is the slowest rate of the successive steps.

The mass loss measured during evaporation of DCM was linear with respect to time during most of the evaporation duration, so that the evaporation rate was constant. The main parameter that influenced the evaporation rate was the stirring process. Indeed the evaporation rates for a given stirring process fall in the same range within experimental accuracy. Thus, the evaporation rate was faster for the more powerful three flat blades propeller than the marine propeller by a factor of ~2 (Table 2). The evaporation rate was controlled by the steps that depended on stirring: the transfer of DCM through the oil–water interface, the transport of DCM in the bulk aqueous phase and the transfer of DCM through the water–air interface.

The transport of DCM in the aqueous phase is given by the "mixing time" of the stirring process. This is defined as the time required for a complete renewal of the liquid in the stirred vessel. This corresponds to the time required for every elementary volume of the fluid passed once at the top surface where evaporation takes place. The "pumping flow rate" of the impeller Q_p (m^3 s^{-1}) is the liquid flow rate through the impeller that depends on the type, diameter, and rotation speed of the impeller. The full circulation rate Q_c (m^3 s^{-1}) containing the flow through the impeller and the back-flow is $Q_p(T/D)^{1/2}$ (Brodkey and Hershey, 1988), so that the mixing time reads

$$t = \frac{V}{Q_c} = \frac{V}{Q_p(T/D)^{1/2}} = \frac{V}{N_q N D^3 (T/D)^{1/2}} \quad (5)$$

where V is the volume of the emulsion (m^3), with N_q the "pumping number" of the impeller, D (m) the diameter of the impeller, T (m) the diameter of the tank, and N the rotation speed (rotations s^{-1}). Taking $N_q = 0.38$ for the three blades propeller and $N_q = 0.50$ for the marine propeller (Roustan, 1991), the mixing times were 1.1 s for the three flat blades propeller and 1.7 s for the marine propeller. Such times were very short as compared to the duration of the evaporation that lasted 20–40 min, showing that the circulation of DCM in the aqueous phase was not the rate-limiting step. The transfer rates through the oil–water and water–gas interfaces took place through stagnant layers that were of the same thicknesses since the stirring was the same at both interfaces. The main difference between the two interfaces was their area. The contact area between the emulsion and the gas phase was the section of the tank, that is, few cm^2. On the contrary the oil–water interfacial area was huge; its order of magnitude was several thousand m^2, depending on the droplet size. The transfer rate through the oil–water interface was much faster than through the water–gas interface. The transfer through the later interface was the rate-limiting step because of its restricted area.

One exception to the general behavior was 80-10-PVA-T that assumed a slower evaporation rate than other samples under stirring with the three flat blades propeller (0.41 g s^{-1} against 0.7–0.9 g s^{-1} for other samples). The oil phase of 80–10-PVA-T was the most concentrated solution (10 wt%) of the highest molar mass PCL. The diffusion of DCM in the very viscous oil phase made the evaporation slower than for other sample where the oil phase was quite fluid. This showed that the composition of the oil phase may contribute to the evaporation rate. Indeed, the diffusivity of DCM is 1.26×10^{-9} m^2 s^{-1} (Lake and Rowe, 2004) against 10^{-10} to 10^{-13} m^2 s^{-1} in a DCM-swollen polymer material (PLGA) (Foss et al., 2009).

3.4. Characterization of the emulsion parameters

Emulsification depended on the stirring process and the physicochemical properties of the materials. The Reynolds number *Re* and Weber number *We* of the flow were calculated from the characteristics of the impellers and the physicochemical properties of the continuous phase according to Eqs. (6) and (7).

$$Re = \frac{\rho_c N D^2}{\eta_c} \quad (6)$$

$$We = \frac{\rho_c N^2 D^3}{\gamma} \quad (7)$$

where N and D are the rotation rate (s^{-1}) and diameter (m) of the impeller, ρ_c and η_c are, respectively, the density (kg m^{-3}) and viscosity (Pa s) of the continuous phase, γ is the interfacial tension (N m^{-1}). The viscosity of continuous phase (η_C) was taken as the viscosity of a 1% PVA solution, 1.2 mPa s. The interfacial tension between DCM and aqueous phase containing only PVA was 4.0 mN m^{-1}, whatever the concentration of PCL in DCM.

The Reynolds numbers *Re* indicated that the emulsions flowed in a turbulent manner since *Re* was higher than 10^4 ($Re = 1.0 \times 10^4$ and $Re = 1.9 \times 10^4$ for the marine propeller and the three blades propeller, respectively). Since the flow was turbulent, the Weber number that is a dimensionless ratio of the initial forces to the interfacial forces was the relevant parameter to be considered as controlling the droplet sizes. The Weber numbers were high ($We = 950$ and $We = 3300$ for the marine propeller and the three

Table 3
Effect of the PCL concentration and molar mass on the organic phase viscosity.

PCL molar mass (Da)	PCL/DCM ratio (wt%)	Viscosity (mPa s)
45,000	3.3	3.5 ± 0.1
45,000	10	30.8 ± 0.3
80,000	3.3	21.6 ± 0.2
80,000	10	528.5 ± 4

blades propeller, respectively), which indicated that the fragmentation of oil droplets by inertial forces was operative.

The droplet size depended on the viscosity of the oil dispersed phase η_D (Fig. 5). Such viscosity dependence operates when the viscous oil resists against droplet fragmentation taking place during short collisions between droplets and turbulent eddies. In particular, the concentrated solution of PCL_{80000} in DCM gave large droplets because it was highly viscous. In the limit of large viscosity of the oil phase, Calabrese et al. (1986a) and Wang and Calabrese (1986) have shown that the droplet diameters varied as $\eta_D^{3/4}$. The viscosities of the emulsion oil phases were measured as reported in Table 3. For fluid oils, the droplet diameter is almost independent of the viscosity of the dispersed phase, in agreement with the large theoretical background developed under the assumption of inviscid oil conditions (Leng and Calabrese, 2004). The present experimental data followed these trends (Fig. 5).

In the limit of low viscosity of the oil phase where the droplet diameter does not depend on η_D, the droplet diameter is related to the size of the turbulent eddies in a straightforward manner. Thus, the specific mean power dissipated in the emulsion of mass M is calculated from the characteristics of the impeller through its power number N_P as

$$\text{mean specific power density} : \varepsilon = \frac{N_P \rho_c N^3 D^5}{M} \quad (8)$$

The mean specific power dissipated by the impeller was $\varepsilon = 0.06\ W\ kg^{-1}$ for the marine propeller using $N_p = 0.4$ (Kato et al., 2009) and $\varepsilon = 1.4\ W\ kg^{-1}$ for the three flat blades propeller using $N_p = 1.5$ (Bates et al., 1963). The size of the smallest turbulent eddies called Kolmogorov microscale λ corresponds to the diameter of the largest droplets that could be fragmented by eddies

$$\text{Kolmogorov microscale} : \lambda = \left(\frac{\eta_c^3}{\varepsilon \rho_c^3}\right)^{1/4} \quad (9)$$

λ corresponds to the diameter of the largest droplet in the emulsion d_{max}; it is conveniently compared to the $d(90)$ of the droplet size distribution of the emulsion. It has been frequently observed that the mean Sauter diameter d_{32} and the maximum diameter d_{max} were proportional (Calabrese et al., 1986b). Their ratio has been estimated from a compilation of experimental values as

$$d_{32} = 0.6 d_{max} = 0.6\lambda \quad (10)$$

As shown in Fig. 5, the droplets diameter for oil phases of low viscosity indeed nicely agreed with the predictions based on the size of Kolmogorov eddies. An upwards departure at high oil viscosities was observed, which was compatible with the slope 3/4 inferred for highly viscous oil phases. The crossover from the low viscous behavior to the high viscosity regime took place at $\eta_D \approx 10$ mPa s. At the end, the droplet sizes can be predicted from the stirring parameters of the process and the viscosities of the dispersed and continuous phases.

3.5. Effect of the stirring process

The marine propeller was less powerful at emulsification than the three flat blades propeller, so that the emulsion droplets and microspheres were larger with the former impeller than the later (Table 1). That the lowest shear stresses caused the largest departure from the expected smooth surface state could be felt a paradoxical result. Indeed the emulsion droplets of large sizes resulting from low shear turned into microparticles with morphological deteriorations upon solvent evaporation. This is in accordance with previous works that have noticed such degradation but did not elucidate their origin (Dubernet et al., 1987). For the same formulation composition, the use of a marine propeller deteriorated the surface state to a larger extent than the three flat blades propeller. Using the marine propeller, scars, defects and holes were observed for the PCL_{45000} and rough microparticles were obtained for the PCL_{80000}. Conversely, small microparticles with a smooth surface were obtained for PCL_{45000} at 3.3 wt% using the three flat blades propeller. It appeared clear from the present results that the coalescence taking place during the solvent evaporation stage was the main origin of surface defects. Since the stirring process was the same during emulsification and solvent evaporation, the stirrer probably played its role on the surface morphology of microparticles during solvent evaporation.

3.6. Effect of the polymer molar mass and concentration in the oil phase

The viscosity of the emulsion oil phase increased with respect to the PCL concentration and molar mass (Table 3), resulting in larger emulsion droplets and larger microparticles sizes as reported in Figs. 2 and 5. Such trends were in agreement with previous reports (Dubernet et al., 1987; Rodriguez et al., 1998; Youan et al., 2001; Lee et al., 2000).

The oil phase viscosity had a direct influence on the morphology. Indeed, microparticles surface states were smooth at low

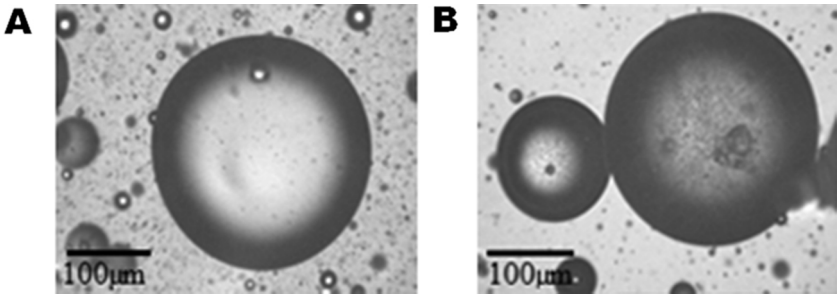

Fig. 5. Variation of the mean droplet diameter d_{32} with respect to the viscosity of the oil phase η_D for the three flat blades propeller (blue circles) and the marine propeller (red squares). The dashed lines mark the prediction of the limiting droplet size for inviscid oil calculated from the Kolmogorov microscale (Eqs. (6) and (7)). The solid line of slope 3/4 is the limiting behavior for highly viscous oils (For interpretation of the color information in this figure legend, the reader is referred to the web version of the article.).

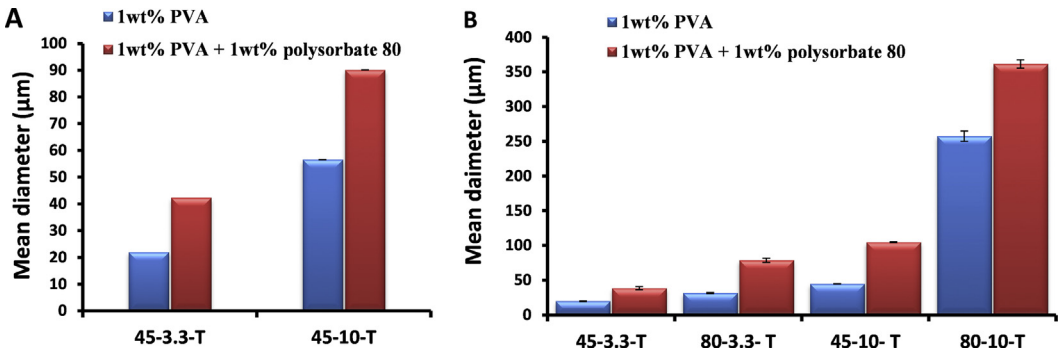

Fig. 6. *In situ* pictures recorded with the video probe for the 80-10-PVA-T experiment: (A) emulsification step, (B) evaporation step (For interpretation of the color information in this figure legend, the reader is referred to the web version of the article.).

Table 4
Interfacial tensions between DCM and aqueous phases of different surfactant compositions.

	No surfactant	1 wt% polysorbate 80	1 wt% PVA + 1 wt% polysorbate 80	1 wt% PVA
Interfacial tension (mN m^{-1})	29.1 ± 0.2	16.4 ± 0.1	13.0 ± 0.1	4.0 ± 0.1

polymer concentration and high shear stirring both for PCL_{45000} and PCL_{80000}. At higher polymer concentrations, degradations of the microparticles surface occurred, the final morphology depending on the PCL molar mass: the microspheres of PCL_{45000} showed scars, defects and holes whereas those of PCL_{80000} were characterized by rough surfaces (Fig. 2). A PCL_{45000}/DCM ratio of 20 wt% led to large particles of 136 μm with holes on their surface and their cross sections of freeze-fractured microparticles clearly showed wells connecting a void in the core and the external surface of the microparticles. The use of PCL_{80000} at the PCL/DCM ratio of 3.3 wt% caused the production of twice larger smooth microparticles as for PCL_{45000} at the same concentration. The large PCL_{80000}/DCM ratios of 10 and 20 wt% caused larger microspheres having increasingly rough surface states. It was noticed that for the highest PCL_{80000}/DCM ratios (10 and 20 wt%), the background of the video probe pictures recorded during the emulsification step was darker than for other samples. Such dark background revealed the presence of small droplets of sizes smaller than the resolution of the camera. As the evaporation proceeded, the background turned clearer and small microparticles could be observed on the surface of large microparticles (Fig. 6). Such observations confirmed the coalescence of small droplets onto larger ones that led to the formation of a rough surface of the final microparticles in case of arrested coalescence.

3.7. Effect of the type of surfactant

As previously mentioned PVA and polysorbate 80 are commonly used stabilizers for oil in water emulsions in general and for the microencapsulation processes in particular. It is expected that a larger concentration of emulsifier causes the formation of smaller emulsion droplets. However, the addition of 1 wt% polysorbate 80 to the previous aqueous phase containing 1 wt% PVA resulted in an increase in the size of the primary emulsion (Fig. 7A) and of the final microspheres (Fig. 7B). In order to find a rationale to such a surprising behavior of polysorbate 80, interfacial tensions and partition coefficients of polysorbate 80 between water and DCM were measured. The interfacial tension between the PCL solution in DCM and the aqueous phase containing 1 wt% polysorbate 80 was 16.4 mN m^{-1}, lower than 29.1 mN m^{-1} obtained without surfactant, but larger than the interfacial tension of 4.0 mN m^{-1} obtained for an aqueous phase containing 1 wt% PVA alone (Table 4). The presence of polysorbate weakened the surface active properties of PVA since the interfacial tension measured for the mixed solution 1 wt% polysorbate 80 + 1 wt% PVA was 13.0 mN m^{-1}. The partition coefficient of polysorbate 80 between water and DCM was 1.57 (Table 5). Thus, for the present emulsions containing 10% oil phase, 15% of the full polysorbate 80 was present inside the oil droplets. On the contrary PVA was almost completely present in the aqueous phase. Polysorbate 80 was pretty soluble in DCM; the peculiar behavior of polysorbate 80 in o/w emulsions of DCM was probably caused by the large concentration of polysorbate 80 (1.35 wt%) in the oil phase. This is a specific behavior of DCM as an oil phase since polysorbate 80 is very often used as an emulsifier of o/w emulsions containing more common oils.

The consequence of using 1 wt% of polysorbate 80 and PVA was the formation of damaged microparticles morphologies regardless the composition of the organic phase or the agitation. Indeed, the surface state had irregular shapes with scars, defects, or holes for the PCL_{45000} microparticles and roughness for the PCL_{80000} microparticles (Fig. 2). A typical morphology as dumbbells was also observed with the use of polysorbate 80 as supplementary emulsifier (45-10-P80-T). Such dumbbells are definitely the mark of an arrested coalescence phenomenon. Coalescence phenomena were observed *in situ* by the video probe in experiments using polysorbate 80 (Fig. 4).

3.8. In vitro drug release behavior of PCL microparticles

The influence of the PCL microparticles morphology on the bioavailability of drugs was assessed by drug release experiments from microparticles having different surface states. The PCL microparticles were loaded with 2 wt% of cholecalciferol (Table 6). Microparticles having their diameters of the same magnitude have been selected because drug release is obviously related to the specific area, that is, to the size of the microparticles (Sansdrap and Moës, 1993). The release behavior for the PCL_{45000} microparticles of 136 μm with holes has been compared to microparticles with scars and defects of 132 μm (Fig. 8A). For the PCL_{80000}

Table 5
Polysorbate 80 and PVA partition coefficient measurement between water and DCM.

	Polysorbate 80 (wt%)	PVA (wt%)
Water phase	38.6 ± 0.8	99.5 ± 0.8
DCM phase	60.6 ± 0.5	
Partition coefficient	1.57	5×10^{-3}

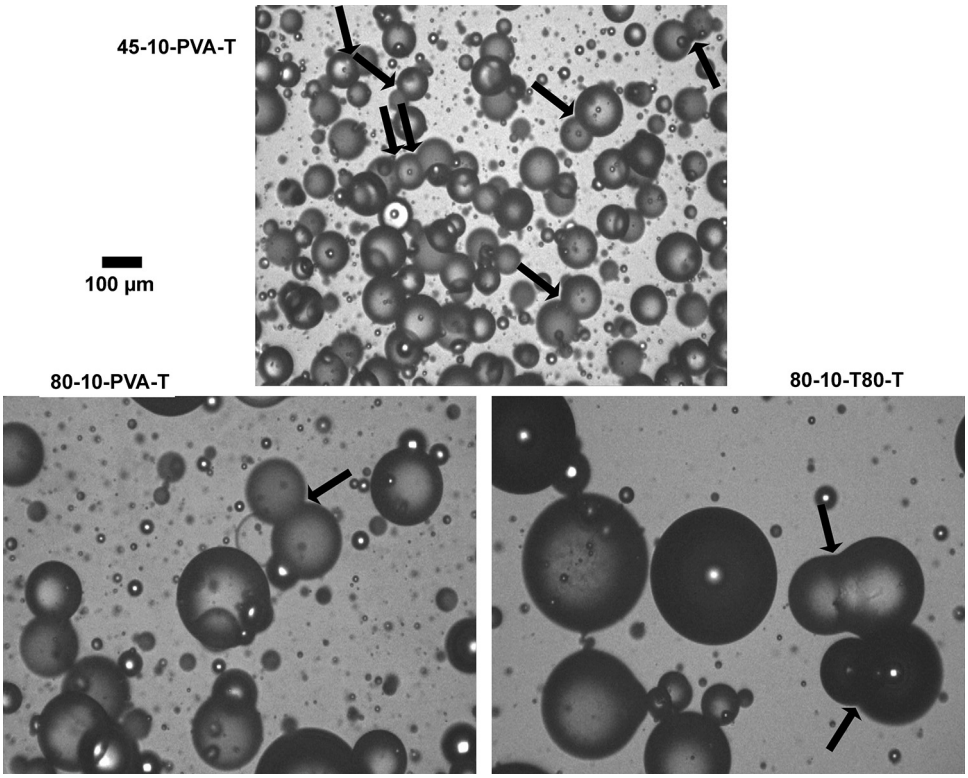

Fig. 7. Effect of the addition of polysorbate 80 on the mean diameter of PCL microparticles: (A) emulsion droplets; (B) microparticles.

Table 6
Drug release experiments: microspheres size, drug loading, Higuchi's release rate constant, and surface state morphology.

Microparticle	Particle size (µm)	Drug loading capacity (wt%)	Encapsulation efficiency (%)	Higuchi rate constant, k_H (wt% $h^{-1/2}$)	Morphological characteristics
45-10-PVA-M	132 ± 5	1.9 ± 0.1	79.6 ± 0.3	1.6	Surface state with scars and defects
45-20-PVA-T	136 ± 5	2.2 ± 0.1	84.4 ± 0.2	3.4	Surface state with holes
80-3.3-P80-M	250 ± 1	2.1 ± 0.1	82.5 ± 0.5	0.53	Relatively smooth surface state
80-10-PVA-T	257 ± 4	2.4 ± 0.1	89.7 ± 0.4	1.0	Rough surface state

microparticles, the drug release from smooth and rough microparticles of 250 and 257 µm, respectively, has been studied (Fig. 8B). In every experiment a burst effect was observed followed by a slower drug release with different profiles depending on the morphology.

The *in vitro* cholecalciferol release behavior was modeled as a passive diffusion from the microparticles into the aqueous continuous phase using the Higuchi model. The cumulated amount of released drug Q increased as the square root of time as

$$Q = k_H t^{1/2} \quad (11)$$

where k_H is the Higuchi's rate constant (Dash et al., 2010). Indeed a plot of Q against $t^{1/2}$ (Fig. 9) was linear during the first 10 h of the release process ($r^2 > 0.99$ in linear regressions), showing that the drug release took place by passive diffusion. The Higuchi rate constant k_H was calculated from the slope (Table 6). The drug release was faster for microparticles of PCL_{45000} with holes ($k_H = 3.4$ wt% $h^{-1/2}$) than for those with scars and defects ($k_H = 1.6$ wt% $h^{-1/2}$). The rough microparticles of PCL_{80000} resulted in faster release ($k_H = 1.0$ wt% $h^{-1/2}$) than the smooth ones ($k_H = 0.53$ wt% $h^{-1/2}$). The release kinetics departed from the

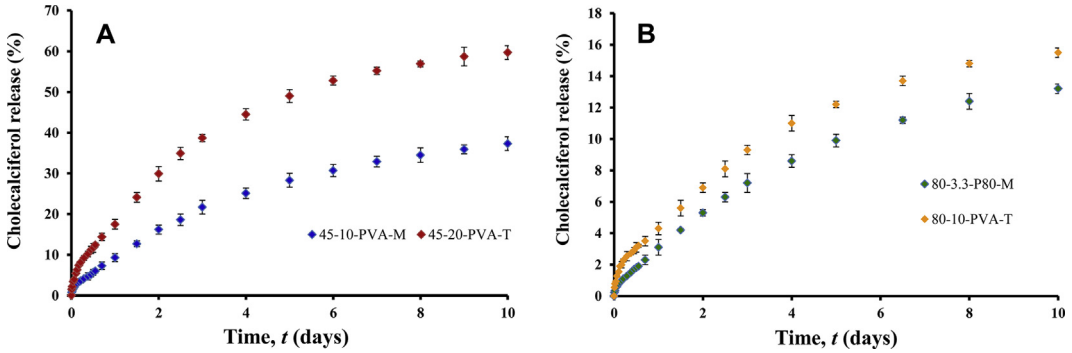

Fig. 8. Release profiles of cholecalciferol from microparticles of different morphologies ($n = 3$): (A) Microparticles of PCL_{45000}; (B) microparticles of PCL_{80000} (For interpretation of the color information in this figure legend, the reader is referred to the web version of the article.).

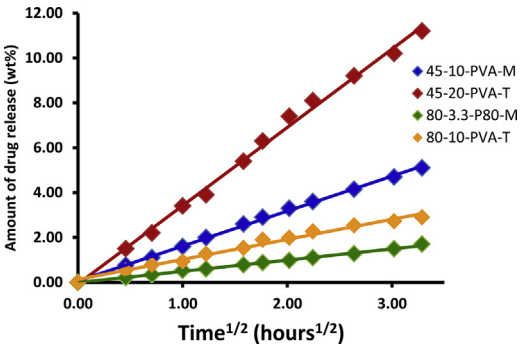

Fig. 9. Results of the Higuchi's model applied on the drug release experiments (For interpretation of the color information in this figure legend, the reader is referred to the web version of the article.).

$t^{1/2}$-dependence for longer times; such departure from Higuchi's behavior was an acceleration of drug release, showing that a supplementary release mechanism was operating for release durations longer than 10 h.

4. General discussion

Few researches concerning the microspheres surface morphology prepared by means of the microencapsulation by the o/w emulsion/solvent evaporation process have been done although such morphology plays an important role in the final drug release profile (Le Ray et al., 2003; Kishida et al., 1990; Freiberg and Zhu, 2004; Yang et al., 2001). The present work has identified the key steps and the several parameters that control the final surface state for the commonly used PCL microparticles. Different morphologies of microparticles have been obtained: the surface state went from spherical and smooth to damaged (Table 2) depending on the process parameters and formulation. Scars and defects, holes as well as roughness were major morphologies raised in this work; they were corresponding to those reported in literature (Jeong et al., 2003; Dubernet et al., 1987; Suave et al., 2010; Dordunoo et al., 1995; Perez et al., 2000; Zhu et al., 2005). Departures from a smooth surface have often been termed as "damaged surface". This is actually a misleading terminology since those different morphologies can be mastered in order to have a control over the drug delivery properties of the microparticles.

All phenomena of relevance regarding the surface morphology of microparticles took place during the solvent evaporation stage. Therefore, the two main hypothesized mechanisms driving the morphology of the particles were the rate of DCM evaporation relative to the rate of droplet coalescence, and the formation of a rigid crust of polymer at the surface of the drying droplets. Evidence of coalescence has been given by several experiments: rough and dumbbell morphologies of the microparticles, larger dry microparticles than expected on the basis of emulsion droplet sizes, and direct observation of coalescence events with the in situ video probe. Full coalescence led to smooth surface of the final microparticles. Arrested coalescence led to the formation of either rough surface morphologies or surface scars corresponding to incomplete healing after arrested coalescence. Holes and cracks came from the rupture of a rigid crust of dry polymer that formed when the oil phase was highly viscous; large voids were left beneath the holes and cracks. All parameters that influence the rates of evaporation and coalescence are of relevance to the control of the morphology. It is noticed that such parameters also influence other phenomena that are not of relevance in the present case, so that bare correlations between physicochemical parameters and final results may be really misleading. The agitation process first, but also, the molar mass of PCL, the polymer concentration in the oil phase, and the use of various surfactants have been identified as playing a key role in the formation of irregularities at the surface. The present results have shown that coalescence during solvent evaporation was the major process of emulsion alteration. Owing to the rather high solubility of DCM in water, Ostwald ripening should obviously operate and it is difficult to figure out how much would be the contribution of Ostwald ripening. The emulsification stage yielded o/w emulsions that did not show so much specific behavior. O/w emulsions containing DCM in the oil phase were of poor stability because the emulsifier did not stabilize oil droplets to high efficiency. The PVA emulsifier has better been selected at optimum with regards to the stability of the final aqueous suspension of polymer microparticles and its tight binding to the surface of PCL microparticles for the emulsifier did not leach into the aqueous phase during utilization.

4.1. Influence of the solvent evaporation rate

The solvent evaporation rate was the main parameter that controlled the surface morphology. Solvent evaporation caused the hardening of the emulsion droplets. Fast hardening quenched transient morphologies of coalescence taking place throughout the solvent evaporation stage. The morphology was under control of the relative rates of coalescence and droplet hardening. It has been found that the solvent evaporation rate was mainly controlled by the type of agitation operating during the evaporation stage. The solvent evaporation rate was influenced by the diffusion of DCM out of the emulsion droplets only in extreme cases where the viscosity of the oil phase was very high. This is in accordance with previous works proving that by using fluid organic phases with lower polymer/solvent ratios the solvent removal was more uniform and faster compared to higher ratios (Li et al., 1995a,b).

4.2. Influences of polymer concentration and molar mass and impact of the agitation system on morphologies

The most obvious consequence of increasing the molar mass or concentration of PCL in the organic phase is an increase of the viscosity of the disperse emulsion phase. It is well-documented that the emulsification of viscous oil phases as o/w emulsions is difficult and results in oil droplets of very large size. However, the size of emulsion droplets was not a parameter of relevance in the present case since the various surface states form during the solvent evaporation stage as a result of the competition between coalescence and solvent evaporation. Solvent evaporation rate was primarily controlled by the stirring rate, except for very viscous oil phases. Coalescence took place in every instance, even in cases where the final microparticles had a smooth surface.

Smooth surface states were obtained with small and fluid emulsion droplets through a low PCL mass or molar mass in the organic phase and through high shearing emulsification process (three flat blades propeller). In those cases coalescence of the fluid emulsion droplets could go to completion, leading to spherical droplets and smooth spherical dry microparticles.

Scars appeared as long lines going all around the particles, resulting in a shape looking as for an apricot. The surface states *with scars and defects* were observed for PCL_{45000} microparticles from 50 to 150 μm mean diameter obtained with an increase in the organic phase viscosity (ratio of 10 wt%) or with a decrease in the shear forces of the agitation system (marine propeller). Coalescence has been arrested because reshaping the emulsion droplets into smooth spheres after a starting coalescence event has been stopped by the early hardening of the droplets. This typical morphology found in the literature (Dubernet et al., 1987; Sato et al., 1988; Jalil and Nixon, 1990; Jeong et al., 2003) showed two or more microparticles stuck together and flattened. Jeffery et al. (1991) argued that high organic phase viscosity obtained by

increasing the polymer concentration may lead to an increased frequency of collisions, resulting in deteriorated morphologies with fusion of semi-formed particles as observed in the present work (45-10-PVA-T). The morphological damages referenced as scars and defects seemed to be the consequence of two or more droplets of same (scars) or different (defects) sizes undergoing coalescence together at an advanced stage of the evaporation and hardening without relaxing their shapes to spheres.

The *rough morphology* observed with viscous solutions of PCL_{80000} at 10 and 20 wt% concentration in DCM showed pieces of small particles stuck to the surface of large microspheres, giving particles looking as a raspberry. This type of morphology was also observed by Suave et al. (2010) with the same polymer. Applying the same deteriorations mechanism as the one used to explain the defects, the roughness of microparticles obtained from the viscous organic phase containing PCL_{80000} seemed to come from small microspheres stuck to the surface of a bigger one. Indeed very small droplets are often present in emulsions. They are formed during the emulsification process when droplets undergo fragmentation into several daughter droplets having the typical size of the turbulent eddies. Fragmentation of large droplets leaves very small satellite droplets in between the main daughter droplets. The formation of satellite droplets is particularly significant for viscous oil phases (Tcholakova et al., 2007). This hypothesis is in agreement with the observations realized *in situ* with the video probe presented in Fig. 5 showing a lot of small droplets in suspension before evaporation that could stick and undergo coalescence at the surface of larger particles at the end of the evaporation stage.

Surface states with holes were observed for the large microparticles above 150 μm obtained by the use of either a high PCL_{45000} concentration of 20 wt% or low shear agitation. Similar morphologies have been found in the literature for microparticles using PCL as polymer matrix (Dordunoo et al., 1995; Perez et al., 2000; Dubernet et al., 1987; Zhu et al., 2005). Holes were presumed to be the result of cracks opened in a rigid crust of PCL formed at the surface of the particles before DCM evaporation reached completion. The formation of such a crust required a concentration gradient of DCM from the center to the surface of the oil droplets. The surface of the droplets depleted in DCM hardened before the DCM present in the core of the droplets could diffuse to the surface. A radial concentration gradient of DCM established inside the droplets when the oil phase was so viscous that the diffusion of DCM to the surface was slower than the evaporation rate of DCM. This is in good agreement with previous work showing that at high polymer concentration the organic phase exhibits an uneven distribution of solvent composition with a rapid hardening of the periphery of the microsphere creating a rigid cortical layer (Li et al., 1995a,b). As the evaporation of the solvent in the aqueous phase proceeded, a difference of osmotic pressure between aqueous and organic phase on both sides of the PCL progressively increased. The crust of dry PCL cracked when the stress caused by the osmotic pressure gradient was larger than the tensile strength of the crust. No hole was drilled for small microparticles because DCM diffused quickly to the surface. For larger microparticles a rigid layer containing low amounts of DCM formed at the surface, while the core of the microparticles still contained solvent that needed to be removed. As DCM is an organic solvent with a low vaporization enthalpy $\Delta_{vap}H$ of 27.98 kJ mol^{-1} and a boiling point of 39.9 °C the solvent in the core can be partially or totally liquid or gaseous because the long time agitation process can heat the medium. To equilibrate the osmotic pressure, a crack generated a hole that allowed the internal gas and/or liquid DCM to reach the aqueous phase. The present SEM (45-20-PVA-T) and previous observations (Perez et al., 2000) performed on cross-sections of microspheres clearly showed a well which was the memory of the path by which the residual solvent core reached the aqueous phase. No hole was observed for the microparticles of PCL_{80000} because of the higher inherent tensile strength and the thicker surface crust of hardening droplets compared to the PCL_{45000}.

4.3. Effect of the interfacial stabilization

Polysorbate 80 is often used to stabilize o/w emulsions in the emulsion/solvent evaporation process. Indeed the HLB 15 of polysorbate shows that it is a hydrophilic emulsifier that stabilizes o/w emulsions. It is demonstrated in accordance with previous studies that polysorbate 80 destabilizes the emulsion compared to the PVA and leads to bigger droplets and microsphere sizes (Table 4; Kim et al., 2005; Benoit et al., 1999). The results in Table 5 shows that during the emulsification a major part of the polysorbate 80 was solubilized in the DCM phase. Therefore, in accordance with the Bancroft rule (Bancroft, 1913, 1915) polysorbate 80 should behave as an oil-soluble emulsifier that stabilizes w/o emulsions. Accordingly, the present o/w emulsions were destabilized by polysorbate 80. This is confirmed by the fact that the addition of polysorbate 80 destabilizes the emulsion by increasing the interfacial tensions compared to the PVA alone (Table 4). As a consequence coalescence phenomena observed *in situ* by the video probe competed with the evaporation rate and resulted in damaged morphologies. Lee et al. (1999) and Kawashima et al. (1993) have shown that microspheres coalesced together when the rate of evaporation was too slow. They also showed that when the diffusion rate of solvent was too fast, the solvent might diffuse into the aqueous phase before stable emulsion droplets were formed, causing the aggregation of embryonic microsphere droplets. A typical morphology looking as dumbbells was obtained for microparticles sizes between 100 and 200 μm upon the use of polysorbate 80 as supplementary emulsifier. Dumbbells were not assumed to be representative of the PCL sticky behavior during the evaporation because the microparticles surface was not well defined. Dumbbells were the consequence of arrested coalescence that took place during the late stages of evaporation. Arrested coalescence was observed when DCM evaporation was slow enough for coalescence to take place, but high enough to freeze the coalescence process at its early stages. Thus arrested coalescence was again the result of a competition between the coalescence and the evaporation rate.

4.4. Impact of the surface state on the drug release rate

Drug release can take place by a burst release at very short times, by passive diffusion through the polymer matrix, or by erosion of the polymer material when it is biodegradable. Those phenomena take place on different time scales and the surface state of the microparticles may influence them in different ways. It has been shown that PCL degradation was slow in aqueous medium because of its semi-crystalline state and hydrophobic character (Ha et al., 1997, Lemmouchi et al., 1998). As a consequence, the presumed predominant mechanism of drug release is diffusion through the amorphous part of the polymer matrix (Perez et al., 2000). This hypothesis is correlated with previous results showing that the Higuchi model was valid, indicating diffusion-controlled release mechanism, following Fick's law. The microparticles surface state influences drug delivery in such instance (Yang et al., 2001).

A burst release is often reported in release kinetics from microencapsulated dosage forms. It is presumed being related to the drug located at the surface of the microparticles that is not retained by the encapsulation process (Yan et al., 1994). Such drug molecules are obviously deposited at the microparticles surface when the manufacture process involves a final drying step where drug molecules present in water stay in the dry product but there is no specific interaction with the microparticles. Such burst release of deposited molecules is observed as soon as the microparticles are

redispersed in water. Besides, several possible mechanisms have been proposed as origins of a burst release. Heterogeneous radial distribution of drug within the microparticle or variation of the polymer material properties close to the microparticles surface are two of them. A heterogeneous structure is not mandatory for a burst release is observed however (Huang and Brazel, 2001). The possible burst release is always followed by a slower release stage due to the diffusion of drug into the dense polymer matrix (Spenlehauer et al., 1988). In the present case, the Higuchi behavior was followed since the first data point recorded after 12 min and the plot of the released amount as a function of $t^{1/2}$ nicely extrapolated to zero released amount. Such behavior demonstrated that there was no burst release and that the release at short times (less than 10 h) was cause by passive diffusion. The microparticles of PCL_{45000} having morphologies with holes did not show a burst release although large craters were present on their surface; showing that even a strongly damaged surface state did not cause encapsulation failure of part of the drug. They had a faster release profile than for the microparticles showing scars and defects however.

The diffusion controlled release following Higuchi model was strongly dependent on the morphology of microcapsules. This was revealed by the Higuchi rate constant k_H value twice higher or more for 45-20-PVA-T than for other microparticles. This is explained by the fact that holes increased the effective surface area of the microparticles promoting exchanges with the aqueous medium and a faster drug release (Gautier et al., 1998; Das and Das, 1998). Moreover, characterization of the PCL_{45000} microparticles with holes showed that the polymeric matrix had macroporous internal and external structures. These interconnected craters enhanced the water penetration into the polymer matrix, the water-filed channels allowing cholecalciferol dissolution and diffusion to the external medium (Le Ray et al., 2003; Vasudev et al., 1997). The present results were in accordance with previous works showing that microparticles containing holes and pores allowed faster drug release compared to smoother ones (Freiberg and Zhu, 2004; Yang et al., 2001). For PCL_{80000}, the rough microparticles resulted in faster release rate than smooth ones as revealed by their Higuchi's k_H values ~2 times higher. Indeed, roughness came from small microparticles stuck to the surface of larger ones during the evaporation step and subjected to arrested coalescence. The contact surface between such stuck microparticles left passages that did not heal forming interconnected channels in which water may easily penetrate, causing in an increase in the cholecalciferol release rate (Yang et al., 2001). As a whole, the accelerated release observed in the diffusion regime was caused by surface defects, but the kinetic release data alone data cannot discriminate the mechanisms. Two main types of accelerated release operated: faster release because of large surface area coming from holes and the irregular shape, and fast release by diffusion through preferential diffusion paths corresponding to pores, defects and incompletely healed scars. The mechanism of release is passive diffusion in any case, so that the Higuchi's law is followed.

There was departure from the Higuchi's law for durations longer than 10 h. The drug release was faster than predicted from the Higuchi's law determined in the short release time regime. Therefore, a supplementary phenomenon causing drug release was operating at long times. Since PCL is a biodegradable polyester, the hydrolysis of the polymer material was probably the origin of the accelerated release. It was indeed claimed that PCL biodegradable was slow and could be neglected in many instances (Ha et al., 1997; Lemmouchi et al., 1998). But the release experiments lasted for very long time, much longer than many experiments reported in the literature. It is therefore likely that the erosion of microparticles by hydrolysis of PCL was the cause of accelerated drug release. Such erosion also depends on the morphology of the microparticles. Thus, the microparticles with holes (45-20-PVA-T) showed a larger acceleration at long times than all other microparticles. The effect of the surface morphology on the release driven by PCL erosion was not significantly different between other microparticles (scary, rough, smooth).

Therefore, the effects of the surface morphology of microparticles was multifold since the surface morphology affected the surface area available for drug transfer to the aqueous solution, the diffusion through structural defects acting as preferential diffusion paths, and the erosion of the polymer material.

5. Conclusion

This study has demonstrated that the morphology of PCL microparticles was highly influenced by the formulation and process parameters of the emulsion-solvent evaporation process. The phenomenon controlling the surface morphology is the competition between droplet coalescence and solvent evaporation driving particles hardening. The picture that emerged from the present investigation is that the morphology of microparticles was controlled by the evaporation rate that represented the time during which the hardening droplets are prone to deformations. As a consequence, there is a competition between the solvent evaporation rate and the rate of the surface state modifications coming from coalescence of emulsion droplets. Fast evaporation enabling the production of smooth microparticles requires a low viscosity of the polymer solution in DCM and high shear rate agitation with efficient stabilizing surfactant. The main parameter of relevance was the stirring process, but other parameter pertaining to the formulation also mattered. The size and the viscosity of the primary emulsion were characteristics of high relevance. As a consequence, attention should be paid to the concentration and molar mass of the polymer in the oil phase, and the stabilization of the primary emulsion with appropriate surfactant. The impact of the surface state on the drug release has also been experimented with cholecalciferol loaded microparticles. It has been found that the surface state strongly influenced drug delivery by PCL microparticles. Thus this study highlighted the importance of the selection of appropriate conditions in order to obtain the desired morphology governing the drug delivery. It is worth noticing that in some works the use of viscous organic phase is necessary in order to increase the encapsulation efficiency (Rafati et al., 1997; Jeong et al., 2003; Kim et al., 2005). This constraint is a limitation that makes difficult to obtain small microparticles sizes with a smooth surface. As a consequence, under such conditions, the simultaneous control of the drug loading and of the microparticles morphology looks a difficult task. A suitable choice of the surface morphology is a way to control drug delivery.

Acknowledgments

This work was done thanks to the financial support from the Fond Unique Interministériel under the project FUI STABIPACK. The authors are also grateful to the help of Alain Rivoire and Jean-Marc Galvan for the use of the *in situ* video probe.

References

Ach, D., Briançon, S., Broze, G., Puel, F., Rivoire, A., Galvan, J.-M., Chevalier, Y., 2015. Formation of microcapsules by complex coacervation. Can. J. Chem. Eng. 93, 183–192.
Almouazen, E., Bourgeois, S., Jordheim, L.P., Fessi, H., Briançon, S., 2013. Nanoencapsulation of vitamin D3 active metabolites for application in chemotherapy: formulation study and in vitro evaluation. Pharm. Res. 30, 1137–1146.
Bancroft, W.D., 1913. The theory of emulsification V. J. Phys. Chem. 17, 501–519.
Bancroft, W.D., 1915. The theory of emulsification VI. J. Phys. Chem. 19, 275–309.
Bates, R.L., Fondy, P.L., Corpstein, R.R., 1963. An examination of some geometric parameters of impeller power. Ind. Eng. Chem. Process Des. Dev. 2, 310–314.

Benoit, J.-P., Courteille, F., Thies, C., 1986. A physicochemical study of the morphology of progesterone-loaded poly(D,L-lactide) microspheres. Int. J. Pharm. 29, 95–102.
Benoit, M.-A., Baras, B., Gillbard, J., 1999. Preparation and characterization of protein-loaded poly(ε-caprolactone) microparticles for oral vaccine delivery. Int. J. Pharm. 184, 73–84.
Brodkey, R.S., Hershey, H.C., 1988. Transport Phenomena. A Unified Approach. McGraw-Hill, New York, Chapter 9.
Calabrese, R.V., Chang, T.P.K., Dang, P.T., 1986a. Drop breakup in turbulent stirred-tank contactors. Part I: Effect of dispersed-phase viscosity. AIChE J. 32, 657–666.
Calabrese, R.V., Wang, C.Y., Bryner, N.P., 1986b. Drop breakup in turbulent stirred-tank contactors. Part III: Correlations for mean size and droplet size distribution. AIChE J. 32, 677–681.
Chung, T.W., Huang, Y.Y., Liu, Y.Z., 2001. Effects of the rate of solvent evaporation on the characteristics of drug loaded PLLA and PDLLA microspheres. Int. J. Pharm. 212, 161–169.
Das, S.K., Das, N.G., 1998. Preparation and in vitro dissolution profile of dual polymer (Eudragit™ RS100 and RL100) microparticles of diltiazem hydrochloride. J. Microencapsul. 15, 445–452.
Dash, S., Murthy, P.N., Nath, L., Chowdhury, P., 2010. Kinetic modeling of drug release from controlled drug delivery systems. Acta Pol. Pharm. 67, 217–223.
Dash, T.K., Konkimalla, V.B., 2012. Poly-ε-caprolactone based formulations for drug delivery and tissue engineering: a review. J. Control. Release 158, 15–33.
Dhanarajua, M.D., Sathyamoorthya, N., Sundar, V.D., Suresh, C., 2010. Preparation of poly(epsilon-caprolactone) microspheres containing etoposide by solvent evaporation method. Asian J. Pharm. Sci. 5, 114–122.
Dordunoo, S.K., Jackson, J.K., Arsenault, L.A., Oktaba, A.M., Hunter, W.L., Burt, H.M., 1995. Taxol encapsulation in poly (epsilon-caprolactone) microspheres. Cancer Chemother. Pharmacol. 36, 279–282.
Dubernet, C., Benoit, J.P., Couarraze, G., Duchêne, D., 1987. Microencapsulation of nitrofurantoin in poly(ε-caprolactone): tableting and in vitro release studies. Int. J. Pharm. 35, 145–156.
Foss, W.R., Anderl, J.N., Clausi, A.L., Burke, P.A., 2009. Diffusivities of dichloromethane in poly(lactide-co-glycolide). J. Appl. Polym. Sci. 112, 1622–1629.
Freiberg, S., Zhu, X., 2004. Polymer microspheres for controlled drug release. Int. J. Pharm. 282, 1–18.
Gagnière, E., Mangin, D., Puel, F., Rivoire, A., Monnier, O., Garcia, E., Klein, J.-P., 2009. Formation of co-crystals: kinetic and thermodynamic aspects. J. Cryst. Growth 311, 2689–2695.
Gautier, H., Guicheux, J., Grimandi, G., Faivre, A., Daculsi, G., Merle, C., 1998. In vitro influence of apatite-granule-specific area on human growth hormone loading and release. J. Biomed. Mater. Res. 40, 606–613.
Girault, H.H., Schiffrin, D.J., Smith, B.D.V., 1984. The measurement of interfacial tension of pendant drops using a video image profile digitizer. J. Colloid Interface Sci. 101, 257–266.
Gonnet, M., Lethuaut, L., Boury, F., 2010. New trends in encapsulation of liposoluble vitamins. J. Control. Release 146, 276–290.
Gross, C., Stamey, T., Hancock, S., Feldman, D., 1998. Treatment of early recurrent prostate cancer with 1, 25-dihydroxyvitamin D3 (calcitriol). J. Urol. 159, 2035–2039.
Gupta, K.C., Kumar, M.N.R., 2001. pH dependent hydrolysis and drug release behavior of chitosan/poly(ethylene glycol) polymer network microspheres. J. Mater. Sci. Mater. Med. 12, 753–759.
Ha, J., Kim, S., Han, S., Sung, Y., Lee, Y., 1997. Albumin release from bioerodible hydrogels based on semi-interpenetrating polymer networks composed of poly(ε-caprolactone) and poly(ethylene glycol) macromer. J. Control. Release 49, 253–262.
Huang, X., Brazel, C.S., 2001. On the importance and mechanisms of burst release in matrix-controlled drug delivery systems. J. Control. Release 73, 121–136.
Huang, Y., Li, L., Fang, Y.E., 2010. Self-assembled particles of N-phthaloylchitosan-g-polycaprolactone molecular bottle brushes as carriers for controlled release of indometacin. J. Mater. Sci. Mater. Med. 21, 557–565.
Izumikawa, S., Yoshioka, S., Aso, Y., Takeda, Y., 1991. Preparation of poly(l-lactide) microspheres of different crystalline morphology on drug release rate. J. Control. Release 15, 133–140.
Jalil, R., Nixon, J.R., 1990. Microencapsulation using poly(DL-lactic acid) III: effect of the polymer molecular weight on the microcapsule properties. J. Microencapsul. 7, 41–52.
Jeffery, H., Davis, S.S., O'Hagan, D.T., 1991. The preparation and characterisation of poly(lactide-co-glycolide) microparticles. I: Oil-in-water emulsion solvent evaporation. Int. J. Pharm. 77, 169–175.
Jeong, J.C., Lee, J., Cho, K., 2003. Effects of crystalline microstructure on drug release behavior of poly(ε-caprolactone) microspheres. J. Control. Release 92, 249–258.
Jeyanthi, R., Mehta, R.C., Thanoo, B.C., DeLuca, P.P., 1997. Effect of processing parameters on the properties of peptide-containing PLGA microspheres. J. Microencapsul. 14, 163–174.
Kato, Y., Tada, Y., Takeda, Y., Hirai, Y., Nagatsu, Y., 2009. Correlation of power consumption for propeller and Pfaudler type impellers. J. Chem. Eng. Jpn. 42, 6–9.
Kawashima, Y., Iwamoto, T., Niwa, T., Takeuchi, H., Hino, T., 1993. Role of the solvent-diffusion-rate modifier in a new emulsion solvent diffusion method for preparation of ketoprofen microspheres. J. Microencapsul. 10, 329–340.
Khalil, A., Puel, F., Chevalier, Y., Galvan, J.-M., Rivoire, A., Klein, J.-P., 2010. Study of droplet size distribution during an emulsification process using in situ video probe coupled with an automatic image analysis. Chem. Eng. J. 165, 946–957.
Khalil, A., Puel, F., Cosson, X., Gorbatchev, O., Chevalier, Y., Galvan, J.-M., Rivoire, A., Klein, J.-P., 2012. Crystallization-in-emulsion process of a melted organic compound: in situ optical monitoring and simultaneous droplet and particle size measurements. J. Cryst. Growth 342, 99–109.
Kim, B.K., Hwang, S.J., Park, J.B., Park, H.J., 2005. Characteristics of felodipine-loaded poly(epsilon–caprolactone) microspheres. J. Microencapsul. 22, 193–203.
Kishida, A., Dressman, J.B., Yoshioka, S., Aso, Y., Takeda, Y., 1990. Some determinants of morphology and release rate from poly(L)lactic acid microspheres. J. Control. Release 13, 83–89.
Lake, C.B., Rowe, R.K., 2004. Volatile organic compound diffusion and sorption coefficients for a needle-punched GCL. Geosynth. Int. 11, 257–272.
Lee, J.H., Park, T.G., Choi, H.K., 1999. Development of oral drug delivery system using floating microspheres. J. Microencapsul. 16, 715–729.
Lee, J.H., Park, T.G., Choi, H.K., 2000. Effect of formulation and processing variables on the characteristics of microspheres for water-soluble drugs prepared by w/o/o double emulsion solvent diffusion method. Int. J. Pharm. 196, 75–83.
Lemmouchi, Y., Schacht, E., Kageruka, P., De Deken, R., Diarra, B., Diall, O., Geerts, S., 1998. Biodegradable polyesters for controlled release of trypanocidal drugs: in vitro and in vivo studies. Biomaterials 19, 1827–1837.
Leng, D.E., Calabrese, R.V., 2004. Immiscible liquid-liquid systems. In: Paul, E.L., Atiemo-Obeng, V.A., Kresta, S.M. (Eds.), Handbook of Industrial Mixing: Science and Practice. Wiley-Interscience, Hoboken New Jersey, pp. 639–753, Chapter 12.
Le Ray, A.-M., Chiffoleau, S., Iooss, P., Grimandi, G., Gouyette, A., Daculsi, G., Merle, C., 2003. Vancomycin encapsulation in biodegradable poly(ε-caprolactone) microparticles for bone implantation. Influence of the formulation process on size, drug loading, in vitro release and cytocompatibility. Biomaterials 24, 443–449.
Li, W.I., Anderson, K.W., DeLuca, P.P., 1995a. Kinetic and thermodynamic modeling of the formation of polymeric microspheres using solvent extraction/evaporation method. J. Control. Release 37, 187–198.
Li, W.I., Anderson, K.W., Mehta, R.C., DeLuca, P.P., 1995b. Prediction of solvent removal profile and effect on properties for peptide loaded PLGA microspheres prepared by solvent extraction/evaporation method. J. Control. Release 37, 199–214.
Li, M., Rouaud, O., Poncelet, D., 2008. Microencapsulation by solvent evaporation: State of the art for process engineering approaches. Int. J. Pharm. 363, 26–39.
O'Donnell, P.B., McGinity, J.W., 1997. Preparation of microspheres by the solvent evaporation technique. Adv. Drug Deliv. Rev. 28, 25–42.
Perez, M.H., Zinutti, C., Lamprecht, A., Ubrich, N., Astier, A., Hoffman, M., Bodmeier, R., Maincent, P., 2000. The preparation and evaluation of poly(ε-caprolactone) microparticles containing both lipophilic and hydrophilic drug. J. Control. Release 65, 429–438.
Petritz, E., Tritthart, T., Wintersteiger, R., 2006. Determination of phylloquinone and cholecalciferol encapsulated in granulates formed by melt extrusion. J. Biochem. Biophys. Methods 69, 101–112.
Rafati, H., Coombes, A.G.A., Adler, J., Holland, J., Davis, S.S., 1997. Protein-loaded poly(DL-lactide-co-glycolide) microparticles for oral administration: formulation, structural and release characteristics. J. Control. Release 43, 89–102.
Rodriguez, M., Vila Jato, J.L., Torres, D., 1998. Design of a new multiparticulate system for potential site-specific and controlled drug delivery to the colonic region. J. Control. Release 55, 67–77.
Roustan, M., 1991. Agitation. Mélange. Caractéristiques des mobiles d'agitation. Les Techniques de l'Ingénieur, A5902.
Sansdrap, P., Moës, A.J., 1993. Influence of manufacturing parameters on the size characteristics and the release profiles of nifedipine from poly(DL-lactide-co-glycolide) microspheres. Int. J. Pharm. 98, 157–164.
Sato, T., Kanke, M., Schroeder, H.G., DeLuca, P.P., 1988. Porous biodegradable microspheres for controlled drug delivery. Part 1. Assessment of processing conditions and solvent removal techniques. Pharm. Res. 5, 21–30.
Sinha, V.R., Bansal, K., Kaushik, R., Kumria, R., Trehan, A., 2004. Poly-ε-caprolactone microspheres and nanospheres: an overview. Int. J. Pharm. 278, 1–23.
Spenlehauer, G., Vert, M., Benoit, J.-P., Chabot, F., Veillard, M., 1988. Biodegradable cisplatin microspheres prepared by the solvent evaporation method: morphology and release characteristics. J. Control. Release 7, 217–229.
Suave, J., Dall'Agnol, E.C., Pezzin, A.P.T., Meier, M.M., Silva, D.A.K., 2010. Biodegradable microspheres of poly(3-hydroxybutyrate)/poly(ε-caprolactone) loaded with Malathion pesticide: preparation, characterization, and in vitro controlled release testing. J. Appl. Polym. Sci. 117, 3419–3427.
Tcholakova, S., Vankova, N., Denkov, N., Danner, T., 2007. Emulsification in turbulent flow: 3. Daughter drop-size distribution. J. Colloid Interface Sci. 310, 570–589.
Vasudev, S.C., Chandy, T., Sharma, C.P., 1997. Development of chitosan/polyethylene vinyl acetate co-matrix: controlled release of aspirin-heparin for preventing cardiovascular thrombosis. Biomaterials 18, 375–381.
Wang, C.Y., Calabrese, R.V., 1986. Drop breakup in turbulent stirred-tank contactors. Part II: Relative influence of viscosity and interfacial tension. AIChE J. 32, 667–676.
Wiscke, C., Schwendeman, S.P., 2008. Principles of encapsulating hydrophobic drugs in PLA/PLGA microparticles. Int. J. Pharm. 364, 298–327.
Woodruff, M.A., Hutmacher, D.W., 2010. The return of a forgotten polymer–polycaprolactone in the 21st century. Prog. Polym. Sci. 35, 1217–1256.

Yan, C., Resau, J.H., Hewetson, J., West, M., Rill, W.L., Kende, M., 1994. Characterization and morphological analysis of protein loaded poly(lactide-co-glycolide) microparticles prepared by water-in-oil-in-water emulsion technique. J. Control. Release 32, 231–241.

Yang, Y.Y., Chung, T.S., Ng, N.P., 2001. Morphology, drug distribution and in vitro release profiles of biodegradable polymeric microspheres containing protein fabricated by double emulsion solvent extraction/evaporation method. Biomaterials 22, 231–241.

Youan, B.B.C., Jackson, T.L., Dickens, L., Hernandez, C., Owusu-Ababio, G.J., 2001. Protein release profiles and morphology of biodegradable microcapsules containing an oily core. J. Control. Release 76, 313–326.

Zhu, K.J., Li, Y., Jiang, H.L., Yasuda, H., Ichimaru, A., Yamamoto, K., Lecomte, P., Jerome, R., 2005. Preparation, characterization and in vitro release properties of ibuprofen-loaded microspheres based on polylactide, poly(ε-caprolactone) and their copolymers. J. Microencapsul. 22, 25–36.